Desalination and Water Treatment
www.deswater.com

doi:10.5004/dwt.2017.1716

72 (2017) 182–189
April

TiO_2@ phenyl-functionalized mesoporous silica for removal of bisphenol A from water

Lijun Luo[a,*], Wei Tan[a], Huabin Xong[a], Colin J. Barrow[b], Pei He[c], Wenrong Yang[b], Hongbin Wang[a,*]

[a]*Key Laboratory of Resource Clean Conversion in Ethnic Regions, Education Department of Yunnan, School of Chemistry and Environment, Yunnan MinZu University, Kunming 650500, China, Tel. +8613629452541, Fax +86 871 65910016, email: 10501931@qq.com (L. Luo), Tel. +8618669010092, email: 317266182@qq.com (W. Tang), Tel. +8613708440749, email: 595530820@qq.com (H. Wang)*

[b]*Centre for Chemistry and Biotechnology, School of Life and Environmental Sciences, Deakin University, Waurn Ponds, VIC 3216, Australia, Tel. 86087165910017, email: colin.barrow@deakin.edu.cn (C.J. Barrow), Tel. +61352272932, email: wenrong.yang@deakin.edu.au (W. yang)*

[c]*Key Laboratory of Tobacco Chemistry of Yunnan Industrial Co., Ltd, Kunming, 650231,China, email: hepeisuccess@163.com*

Received 8 December 2015; Accepted 7 July 2016

ABSTRACT

A novel phenyl-functionalized mesoporous silica based on TiO_2 supporter was synthesized to remove bisphenol A (BPA) quickly, which is a representative endocrine disrupting chemical. The prepared sorbents were characterized by nitrogen (N_2) adsorption-desorption measurement (BET) and Fourier transform infrared spectroscopy. The effects of the temperature, initial pH value and initial BPA concentration of solution on the adsorption capacity were investigated. And adsorption behaviors of the adsorbent for BPA, such as adsorption kinetics, isotherms, thermodynamics and effect of coexisting pollutants, were also investigated. The result indicated the maximum adsorption capacity of TiO_2-Mip-Ms (22 mg g^{-1}) is the two times higher than that of TiO_2-Nip-Ms (11 mg g^{-1}), and the Langmuir model fits better than Freundlich model. The adsorption kinetic of BPA onto TiO_2-Mip-Ms and TiO_2-Nip-Ms belonged to the pseudo-second-order kinetic model, and adsorption rate constant of TiO_2-Mip-Ms (0.0156 g mg^{-1} min^{-1}) is near three times than that of TiO_2-Nip-Ms (0.0058 g mg^{-1} min^{-1}). The BPA adsorption onto TiO_2-Mip-Ms was thermodynamically feasible and spontaneous.

Keywords: Mesoporous silica; Adsorption; Bisphenol A; Surface molecular imprinting; TiO_2

1. Introduction

The environmental pollution of endocrine disrupting chemicals (EDCs) in water sources has drawn considerable scientific and public attention over the past decade [1–3] because they can interfere the reproductive system of wildlife and human even at very low concentration (ppb level). Bisphenol A (2,2-bis(4-hydroxyphenyl)propane; BPA), which is one of these EDCs [4–6], has been widely used in the production of polycarbonate plastics, epoxy resins and unsaturated polyester-styrene resins as a monomer. As a result, it was reported that BPA had been widely detected in different water sources, with concentration of 81.77~531.85 ng L^{-1} in water sources, even in the effluents of wastewater treatment plants [7,8]. Therefore, it is urgent to develop an effective and rapid method to remove BPA from water. Physical adsorption is generally regarded as efficient way to remove EDCs because of low cost, easy operation and no producing secondary harmful substances. Activated carbon is a well-known adsorbent of different contaminants [9]. However, it

*Corresponding author.

Presented at the 8th International Conference on Challenges in Environmental Science & Engineering (CESE-2015), 28 September–2 October 2015, Sydney, Australia.

Lijun Luo and Wei Tang contributed equally to this work

has slow adsorption rate and often suffers from pore blocking and a lack of regenerative ability. So it is important to develop fast adsorbents to remove this type of pollutants from water [10]. The molecularly imprinted functionalized materials are considered as a kind of fast adsorbents [11–13].

Mesoporous silica (Ms) is an ordinary adsorbent for many hydrophilic organic contaminants due to their larger surface area, pore size and its hydrophilic nature. In addition, the pore surface of Ms functionalized by anchoring various hydrophobic organic groups by post-synthesis grafting or co-condensation also can be used to remove hydrophobic pollutants [14]. However, the hydrophobic porous silica synthesized by traditional methods exhibits poor site accessibility and slow mass transfer to the target contaminants [15,16]; surface molecular imprinting technology is a good method to prepare fast adsorbent. Titanium dioxide can be used as a supporter of Ms because of its good chemical stability, low cost and nontoxicity [17]. In the present study, we used nano-TiO_2 as a supporter of Ms to prepare TiO_2-mesporous silica (denoted as TiO_2-Ms) hybrid materials by sol-gel method. During the preparation process, hydrophobic phenyl groups were introduced into the Ms to provide hydrophobic sites, which can interact with two benzene rings of hydrophobic BPA through a strong ϖ-ϖ interaction. Moreover, we adopted surface molecular imprinting technique to further enhance the specific surface area of hydrophobic Ms onto the surface of TiO_2. The prepared adsorbents were used to adsorb BPA from wastewater. The adsorption characteristics of BPA from aqueous solutions over the synthesized materials including the effect factors (initial concentration, solution pH and temperature, co-pollutants), adsorption kinetics, adsorption isotherms and thermodynamics were investigated.

2. Materials and methods

2.1. Materials and reagents

TiO_2 particles (P25, ca. 80% anatase, 20% rutile; BET area, ca. 50 $m^2 g^{-1}$) were purchased from Degussa (Germany). Tetraethoxysilance (TEOS; Chengdu Kelong Chemical Reagent Factory, China, 99%), phenyltriethoxysilane (PhTES; Alfa Aesar, 99%), hexadecyltrimethylammonium bromide (CTAB; Aladdin, 99%), BPA (Aldrich, 99%), phenol and 2-Nitrophenol (2-NP; Aldrich, 99%) and the other chemicals were of analytical purity grade (Chengdu Kelong Chemical Reagent Factory, China) without further purification. Stock solution was prepared by dissolving BPA in methanol followed by gradual dilution with ultrapure water to about 20 mg L^{-1}, in which the methanol concentration was about 0.10% (v/v). HPLC-grade acetonitrile was obtained from Merck. Ultrapure water (18.2 MΩ) used throughout the experiments was obtained from laboratory purification system.

2.2. Synthesis of adsorbents

A novel phenyl group functionalized Ms based on TiO_2 particles (denoted as TiO_2-Mip-Ms) was prepared as follows: 0.6 g of CTAB was dissolved in 28 g of hot distilled water (333 K). Then the solution was cooled down, and 2.0 g of 25% ammonia solution was added to adjust the pH value of solution to 11.8. After that, a weighted amount of TiO_2 (Degussa P25, 1.2 g) was dispersed in the solution under vigorous stirring for 2 min followed by treating with ultrasonication for 30 min. In another beaker, 0.6 g of BPA was dissolved in 8 mL of absolute alcohol, and 2.16 g of TEOS and 1.14 g of PhTES were added into it. Then the above-prepared solution was poured into the titanium dioxide suspension under vigorous stirring for 2 min followed by treating with ultrasonication for 30 min, and the mixture solution was aged for 6 h under stirring at room temperature. The resultant white precipitate was filtered, washed with water and ethanol, and dried at 80°C overnight in vacuum. The template CTAB and BPA molecules were removed by suspending solid product in 50 mL of ethanol and 0.15 mol L^{-1} HCl and refluxing at 80°C for 24 h for two times. The final powder product was filtered and washed with ethanol and water until BPA could not be detected, and dried at 80°C for overnight in vacuum. The phenyl group functionalized Ms based on TiO_2 as a supporter was denoted as TiO_2-Nip-Ms in a similar way to that of the TiO_2-Mip-Ms only without adding BPA. TiO_2-Ms was obtained when neither BPA nor PhTES was used in the preparation process.

2.3. Materials characterization

In order to analyze the functional groups in the prepared adsorbents, infrared absorption spectra of adsorbents were conducted on a Nicolet iS10 FT-IR spectrometer (Thermo Scientific, Germany) using KBr pellet technique over the wave number range of 4,000–400 cm^{-1} with a resolution of 2 cm^{-1}. The specific surface area and the pore distribution of adsorbents were measured with TriStar II 3020 surface area measurement instrument (Micromeritics Inc., USA) at 77 K following the BET method.

2.4. Adsorption experiments

2.4.1. Adsorption kinetic study

Adsorption kinetic experiments were performed by batch adsorption method at 298 K on a shaker at 200 rpm. A series of samples were prepared by mixing about 0.0050 g of adsorbents (TiO_2-Mip-Ms, TiO_2-Nip-Ms and TiO_2-Ms) with BPA solution (25.00 mL, 10 mg L^{-1}) in a 25 mL conical flask. Samples were withdrawn at selected time intervals from 0 to 80 min and filtered through a 0.45 μm filter to remove the particles. The exact concentrations of resultant BPA solution were measured by high-performance liquid chromatography (HPLC).

2.4.2. Adsorption isotherm study

Adsorption isotherm experiments were carried out by mixing approximately 0.005 g of adsorbents (TiO_2-Mip-Ms, TiO_2-Nip-Ms and TiO_2-Ms) with 25.00 mL BPA solution in a 50 mL conical flask. The initial concentration of BPA solution was varied in the range of 10–110 mg L^{-1}. To achieve saturated adsorption, the sample solution was shaken continuously at 200 rpm and 298 K for 1 h and filtered with 0.45 μm filter. Then concentration of the BPA was analyzed.

2.4.3. Adsorption thermodynamic study

Adsorption thermodynamic experiment was performed by mixing 25.00 ml BPA (10 mg L^{-1}) with about 0.005 g TiO_2-Mip-Ms in a 50 mL conical flask. And the mixture solutions were shaken at different temperature of 293.15, 313.15 and

333.15 K in a temperature-controlled mechanical shaker (Sukun Sky-200B) for 1 h.

2.4.4. pH study

To order to investigate the effect of pH value of BPA solution on the adsorption capacity, the experiments were carried out by mixing 25.00 mL BPA solution (10 mg L^{-1}) with about 0.005 g TiO_2-Mip-Ms at different pH values of 2, 4, 5, 7, 9 and 12. The initial pH value was adjusted by hydrochloric acid and sodium hydroxide solutions with concentrations of 0.1 mol L^{-1} and measured using pH meter (Shanghai PHS-3B).

2.4.5. The effect of coexisting pollutants on the adsorption capacity for BPA

In order to investigate recognition ability of TiO_2-Mip-Ms for BPA, we selected the PP and 2-NP as coexisting contaminants, The adsorption experiments for BPA were carried out by mixing about 0.005 g adsorbents with 25.00 mL BPA solution with different concentration (10 mg L^{-1}, 80 mg L^{-1}) in the presence of 10 mg L^{-1} phenol or 2-NP (10 mg L^{-1}) in a 50 mL conical flash. To achieve saturated adsorption, the sample solution was shaken at 200 rpm and 298 K for 1 h. The concentrations of adsorbates in solution were analyzed by HPLC.

2.4.6. Calculation of adsorption capacity of BPA

The adsorption capacity was calculated according to the following equation (Eq. (1)).

$$q_e = \frac{(C_0 - C_e)V}{m} \quad (1)$$

where q_e (mg g^{-1}) is the equilibrium adsorption amount; C_0 (mg L^{-1}) is the initial concentration of BPA in the solution; C_e (mg L^{-1}) is the equilibrium concentration of BPA in the solution, V (L) is the solution volume; and m (g) is the mass of the adsorbent.

2.5. Analytical method

At the end of the adsorption experiments, the solution containing the adsorbents was filtered through a 0.45 μm filter to remove the adsorbents. The concentration of BPA, phenol and 2-NP were analyzed by the HPLC (Agilent Technologies 1200series), in which C18 column (Agilent, Eclipse XDB-C18, 4.6 nm × 150 mm, 5 μm) was applied. The running temperature was 35°C, and the injection volume was 20 μL. The UV detector (DAD) wavelength was 226 nm for BPA and phenol, and 278 nm for 2-NP. The mobile-phase composition was acetonitrile/water (45/55, v/v) for BPA/phenol binary solution, and acetonitrile/water (35/65, v/v) for BPA /2-NP binary solution with a flow rate of 1 mL min^{-1}.

3. Results and discussion

3.1. Materials characterizations

In order to ascertain the surface area and pore structure of adsorbents, the N_2 adsorption-desorption isotherms measurement was performed. N_2 adsorption-desorption isotherms for TiO_2-Ms, TiO_2-Mip-Ms, TiO_2-Nip-Ms and P25 at 77 K were shown in Fig. 1(A). The isotherms of TiO_2-Ms (a) is identified as classical type IV by IUPAC, which is characteristic of mesoporous structure. Whereas, TiO_2-Mip-Ms (b) and TiO_2-Nip-Ms (c) showed type I isotherms, which indicated the materials containing microspores. The isotherm of P25 belongs to type III, which is characteristic in a solid happened on weak gas-solid interaction. Corresponding to BJH pore size distribution of TiO_2-Ms (a), TiO_2-Mip-Ms (b), TiO_2-Nip-Ms (c) and P25 (d) were also presented in Fig. 1(B). The maximum pore size of TiO_2-Ms was about 2.6 nm, whereas the pore sizes of TiO_2-Mip-Ms (b) and TiO_2-Nip-Ms (c) were about 2 nm. Table 1 summarizes the physical parameters of the composite materials obtained from the N_2 adsorption-desorption. The TiO_2-Ms showed higher large surface area of 262 m^2 g^{-1} than P25 of 50 m^2 g^{-1}. When phenyl group was introduced into TiO_2-Ms, the surface areas and total pore volume of TiO_2-Mip-Ms and TiO_2-Nip-Ms decreased to 216 and 140 m^2 g^{-1}, respectively. This is because the phenyl functional group

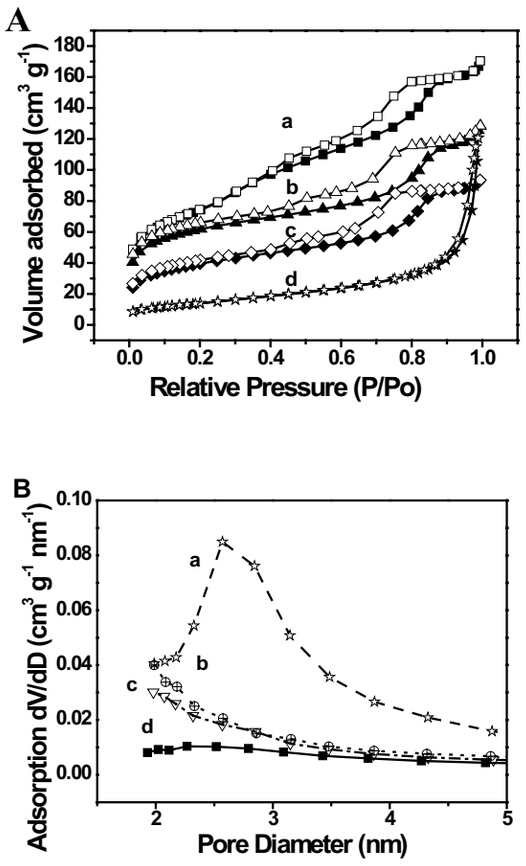

Fig. 1 (A). N_2 adsorption-desorption isotherms and (B) BJH pore size distribution of TiO_2-Ms (a. TiO_2/mesoporous silica), TiO_2-Mip-Ms (b. TiO_2/phenyl group functionalized imprinting mesoporous silica), TiO_2-Nip-Ms (c. TiO_2/phenyl group functionalized non-imprinting mesoporous silica) and P25 (d. open and solid symbols represent desorption and adsorption branches, respectively).

Table 1
BET surface area and pore parameters of TiO_2-Mip-Ms, TiO_2-Nip-Ms, TiO_2-Ms and P25

Adsorbent	Pore diameter (nm)	BET surface area ($m^2\ g^{-1}$)	Total pore volume
TiO_2-Mip-Ms	2.0	216	0.15
TiO_2-Nip-Ms	2.0	140	0.12
TiO_2-Ms	2.6	262	0.25
P25	–	50	–

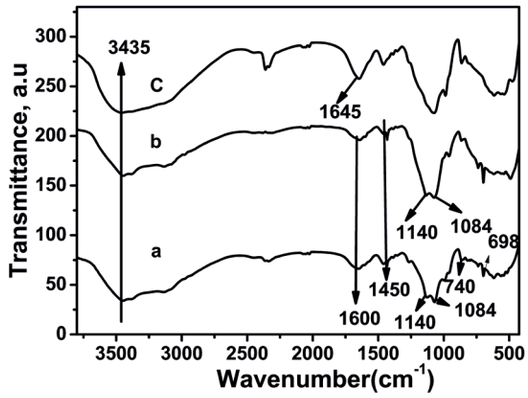

Fig. 2. FT-IR spectra of TiO_2/Nip-MS (a. TiO_2/phenyl group functionalized non-imprinting mesoporous silica) and TiO_2/MS (b. TiO_2/mesoporous silica).

may occupy the internal space of the Ms and made the pores become narrower. The surface area and total pore volume of TiO_2-Mip-Ms were larger than that of TiO_2-Nip-Ms; this phenomenon is attributed to the added BPA during preparation process; BPA may be as a pore expanding agent in this process. In general, the pore diameter should decrease in parallel with the pore volume via modification the organosilanes because the long alkyl chains or other organic groups occupy the internal space of the cavities [18].

To verify the phenyl group has been anchored on the pore surface of Ms successfully. Infrared absorption spectra of TiO_2-Mip-Ms, TiO_2-Nip-Ms and TiO_2-Ms was measured and shown as Fig. 2. It shows that the broad absorption peak of the TiO_2-Mip-Ms, TiO_2-Nip-Ms and TiO_2-Ms near 3435 cm^{-1} is assigned to the stretching vibration of O-H hydroxyl groups. Si-O-Si vibrational mode appears near 460, 870 and 1072 cm^{-1}. Bending vibration and asymmetrical stretch of Si-OH or Ti-OH is at 1635 cm^{-1} and 960 cm^{-1}, respectively. Moreover, TiO_2-Mip-Ms and TiO_2-Nip-Ms showed the characteristic absorption peaks of benzene ring at 698 and 740 cm^{-1} and peak of 1432 cm^{-1} of C=C stretching vibrations. The peak of 1137 cm^{-1} indicated the presence of Si-C bond. Fourier transform infrared spectroscopy spectra confirmed that the phenyl group was successfully anchored into the silicate network.

3.2. The effect factors on the adsorption capacity of BPA on the adsorbents

3.2.1. The effect of contact time on the adsorption capacity on the adsorbents

In order to investigate the adsorption rate of BPA on the adsorbents, the adsorption capacity of BPA as a function of contact time was presented in Fig. 3. The results indicated that the adsorption amount of BPA on TiO_2-Mip-Ms increased faster than that of BPA on TiO_2-Mip-Ms from 0 to 40 min, and the BPA adsorption reached the equilibrium in less than 60 min (Fig. 3); However, the adsorption amount of BPA on TiO_2-Ms was very low and did not change at all from 10 to 60 min.

3.2.2. The effect of solution pH on the adsorption capacity of BPA on the adsorbents

In order to investigate the pH influence on the adsorption capacity of BPA on TiO_2-Mip-Ms and TiO_2-Nip-Ms, the experiment was carried out at different solution pH value ranging from 2 to 12. As shown in Fig. 4, the adsorption amount of BPA on adsorbents exhibited a constant with the

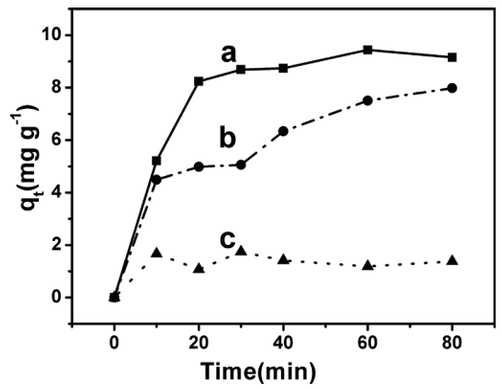

Fig. 3. Adsorption capacities of bisphenol A (BPA) on TiO_2-Mip-Ms (a. TiO_2/phenyl group functionalized imprinting mesoporous silica), TiO_2-Nip-Ms (b. TiO_2/phenyl group functionalized non-imprinting mesoporous silica) and TiO_2-Ms (c. 2 g L^{-1} dosage and 20 mg L^{-1} BPA solution) vs. time.

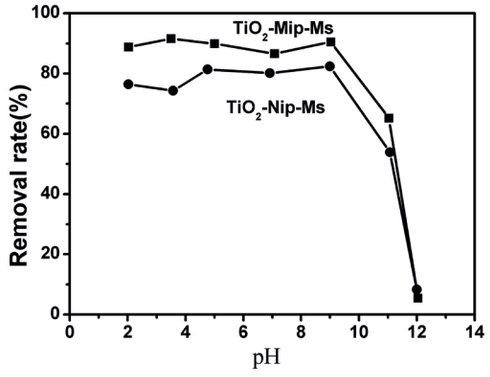

Fig. 4. Effect of solution pH on adsorption capacity of BPA on TiO_2-Mip-Ms (TiO_2/phenyl group functionalized imprinting mesoporous silica) and TiO_2-Nip-Ms (TiO_2/phenyl group functionalized non-imprinting mesoporous silica).

increasing of pH value from 2 to 9, indicating that the binding affinity between BPA and the binding sites did not significantly change under acidic conditions. The adsorption amount of BPA decreased remarkably at a higher pH value ranging from 9 to 11; this phenomenon was observed from other adsorbents, such as activated carbon. The result could be explained by the pKa value of BPA ranging from 9.9 to 10.2, and BPA forms bisphenolate anion, and the electrostatic repulsion between BPA and the sorbent becomes increasingly stronger and overcomes the binding affinity, which led to the adsorption capacity of BPA on the TiO_2-Mip-Ms and TiO_2-Nip-Ms decreased under alkalinity condition.

3.2.3. The effect of initial concentration of BPA on the adsorption capacity

The influence of initial concentration of BPA on the adsorption capacity was investigated with the initial BPA concentration being varied from 10 to 110 mg L^{-1} as shown in Fig. 5. Among these sorbents, the TiO_2-Ms showed very low adsorption capacities for BPA less than 2 mg g^{-1}, because the TiO_2-Ms has a characteristic of hydrophilic nature compared with the TiO_2-Mip-Ms and TiO_2-Nip-Ms. Whereas, the TiO_2-Mip-Ms and TiO_2-Nip-Ms showed higher adsorption capacity for BPA with maximum values of 22 and 11 mg g^{-1}, respectively, which indicated that phenyl groups introduced into the surface of Ms were hydrophobic and had a strong binding ability for hydrophobic BPA. It was interesting to find that the adsorption capacity of BPA onto TiO_2-Mip-Ms was the two times higher than that of BPA on TiO_2-Nip-Ms. This phenomenon could be assigned to the higher specific area surface of TiO_2-Mip-Ms (216 m^2 g^{-1}) than that of TiO_2-Mip-Ms (140 m^2 g^{-1}).

3.2.4. The effect of the temperature of solution on the adsorption capacity

The effect of the temperature on equilibrium adsorption capacity of BPA onto TiO_2-Mip-Ms was studied at 293.15, 313.15 and 333.15 K. The equilibrium adsorption capacity of BPA onto TiO_2-Mip-Ms reduced as the adsorption temperature increased (Fig. 6), which indicated that the binding of BPA was exothermic in nature.

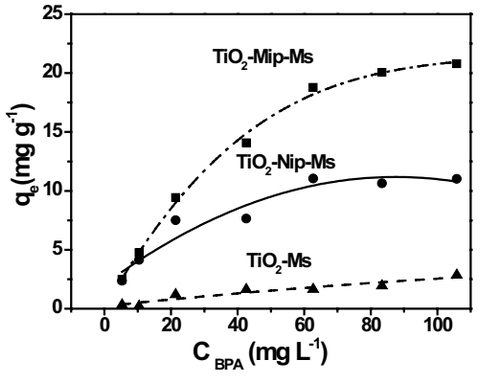

Fig. 5. Effect of initial concentration on adsorption capacity of BPA on TiO_2-Mip-Ms (TiO_2/phenyl group functionalized imprinting mesoporous silica), TiO_2-Nip-Ms (TiO_2/phenyl group functionalized non-imprinting mesoporous silica) and TiO_2-Ms (TiO_2/mesoporous silica).

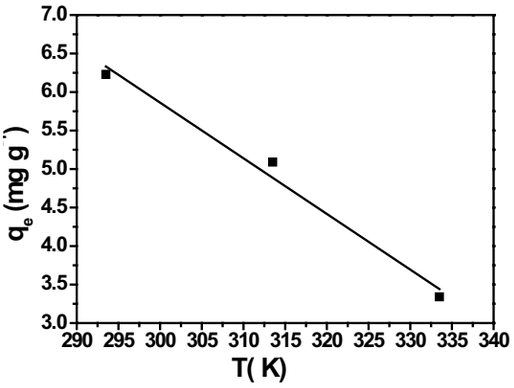

Fig. 6. Effect of temperature of solution on adsorption capacity of BPA on TiO_2-Mip-Ms (TiO_2/phenyl group functionalized imprinting mesoporous silica).

3.3. Adsorption kinetic study

To investigate adsorption characteristics of BPA, adsorption processes were described by both pseudo-first-order kinetics [19,20] (Eq. (2)) and pseudo-second-order kinetics model [21,22] (Eq. (3)) in this work:

$$\ln \frac{(q_e - q_t)}{q_e} = -k_1 t \tag{2}$$

$$\frac{t}{q_t} = \frac{1}{k_2 q_e^2} + \frac{1}{q_e} t \tag{3}$$

where q_e and q_t (mg g^{-1}) is the adsorption amount of BPA adsorbed at equilibrium and at time t, respectively, and k_1 (1 min^{-1}) and k_2 (g (mg^{-1}·min^{-1}) is the pseudo-first-order constant and pseudo-second-order constant, respectively.

The experimental data were fitted with the pseudo-first-order kinetics and pseudo-second-order kinetics equations. The results of fitting the experimental data with pseudo-second-order kinetics model on TiO_2-Mip-Ms and TiO_2-Nip-Ms were shown in Fig. 7. The obtained kinetic parameters for BPA onto TiO_2-Mip-Ms and TiO_2-Nip-Ms were summarized in Table 2. The best-fit model was selected according to linear regression correlation coefficient (R^2) and theoretical $q_{e(cal)}$ value. The pseudo-second-order model for BPA adsorption onto TiO_2-Mip-Ms and TiO_2-Nip-Ms can describe better than the Pseudo-first-order model, because the correlation coefficients R^2 = 0.9920 and 0.9520 of pseudo-second-order model are higher than 0.9670 and 0.9482 of pseudo-first-order model, respectively. Moreover, the $q_{e(cal)}$ value obtained from pseudo-second-order model fitting was closer to the experimental $q_{e(exp)}$ value than the $q_{e(cal)}$ obtained from pseudo-first-order model. Therefore, the adsorption behaviors of BPA onto TiO_2-Mip-Ms and TiO_2-Nip-Ms belonged to the pseudo-second-order kinetic model. It was also observed that adsorption rate constant of BPA on TiO_2-Mip-Ms (0.0156 g mg^{-1} min^{-1}) is near three times than that of BPA on TiO_2-Nip-Ms (0.0058 g mg^{-1} min^{-1}).

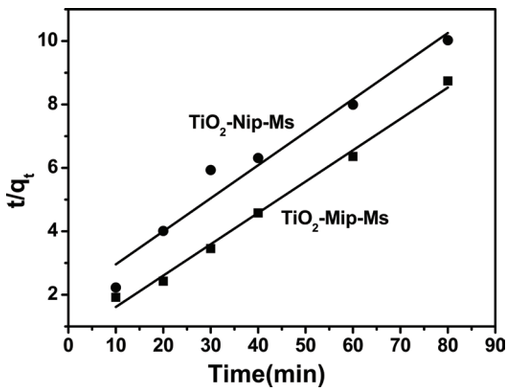

Fig. 7 Pseudo-second-order kinetics plot lines of TiO_2-Mip-Ms (TiO_2/phenyl group functionalized imprinting mesoporous silica) and TiO_2-Nip-Ms (TiO_2/phenyl group functionalized non-imprinting mesoporous silica).

This result can be explained that there are more active sites at the pore surface of TiO_2-Mip-Ms than TiO_2-Nip-Ms.

3.4. Adsorption isotherm study

To understand the adsorbate-adsorbent interactions, we investigated the adsorption isotherms of BPA on the prepared adsorbents. In this work, Langmuir equation (Eq. (4)) and Freundlich equations (Eq. (5)) [23,24] were adopted to simulate the experimental data.

$$\frac{1}{q_e} = \frac{1}{q_m K_L C_e} + \frac{1}{q_m} \tag{4}$$

$$q_e = K_F C_e^{1/n} \tag{5}$$

In Eq. (4), K_L (L mg^{-1}) is the Langmuir constant, which describes the intensity of the adsorption process, and q_m (mg g^{-1}) reflects maximum adsorption capacity. In Eq. (5), K_f is the empirical constant related to bonding energy, which represents the general capacity of BPA adsorbed onto adsorbents for a unit equilibrium concentration. $1/n$, with a range between 0 and 1, reflects adsorption intensity or surface heterogeneity.

The adsorption isotherm parameters were calculated from Langmuir model and Freundlich model and listed in Table 3. The best-fit model was selected according to linear regression correlation coefficient (R^2). It is clear that the Langmuir model fits better than Freundlich model onto TiO_2-Mip-Ms and TiO_2-Nip-Ms, as reflected with correlation coefficients (R^2) of 0.9935 vs. 0.9443, and 0.9808 vs. 0.9206, respectively. The maximum adsorption capacity of TiO_2-Mip-Ms and TiO_2-Nip-Ms for BPA was evaluated to be 21.85 and 11.43 mg g^{-1}, respectively. The higher adsorption capacity of TiO_2-Mip-Ms can be explained that higher specific surface area relative to TiO_2-Nip-Ms. While BPA adsorption on TiO_2-Ms obeyed the Freundilich model, because of higher correlation coefficients (0.9299–0.7731). It indicated that adsorption behavior belonged to homogeneous and monolayer adsorption at the surface of TiO_2-Mip-Ms and TiO_2-Nip-Ms. On the contrary, the adsorption behavior ought to be heterogeneous.

3.5. Adsorption thermodynamics study

The adsorption thermodynamic parameters such as standard free energy change (ΔG°), standard enthalpy change (ΔH°) and standard entropy change (ΔS°) can be estimated with the following equations:

$$\ln k_d = -\frac{\Delta H^\circ}{RT} + \frac{\Delta S^\circ}{R} \tag{6}$$

Table 2
Kinetic parameters for BPA adsorption onto TiO_2-Mip-Ms and TiO_2-Nip-Ms

Adsorbents	Pseudo-first-order kinetics				Pseudo-second-order kinetics		
	κ_1 (min)	$q_{e,cal}$ (mg g^{-1})	$q_{e,exp}$ (mg g^{-1})	R^2	κ_2 (g mg^{-1} min^{-1})	$q_{e,cal}$ (mg g^{-1})	R^2
TiO_2-Mip-Ms	0.069	7.61	9.43	0.9670	0.0156	10.11	0.9920
TiO_2-Nip-Ms	0.042	7.36	8.00	0.9482	0.0058	9.59	0.9520

$q_{e,exp}$: adsorption capacity measured from experiment.
$q_{e,cal}$: adsorption capacity estimated by the kinetic model.
R^2: correlation coefficient.

Table 3
Adsorption isotherm parameters onto TiO2-Mip-Ms, TiO2-Nip Ms and TiO2-Ms

Adsorbents	Langmuir model			Freundlich model		
	q_m	K_L (L mg^{-1})	R^2	K_F	$1/n$	R^2
TiO_2-Mip-Ms	21.85	0.2467	0.9935	4.9102	0.3861	0.9443
TiO_2-Nip-Ms	11.43	0.2210	0.9808	3.4306	0.2828	0.9206
TiO_2-Ms	3.58	0.0203	0.7731	0.1375	0.6425	0.9299

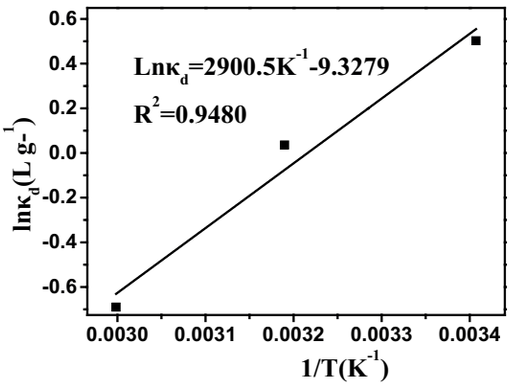

Fig. 8. Linear van't Hoff equation: $\ln\kappa_d$ vs. 1/T (TiO_2/phenyl group functionalized imprinting mesoporous silica).

$$\Delta G^\circ = \Delta H^\circ - T\Delta S^\circ \quad (7)$$

where R is the universal gas constant, and T (K) is the temperature. Moreover, K_d is the distribution coefficient calculated using the below equation [25]:

$$K_d = \frac{q_d}{C_e} \quad (8)$$

In this work, the distribution coefficient (κ_d) was evaluated in the range of 293.15–333.15 K according to Eq. (8). The van't Hoff equation linearization given by the plot $\ln\kappa_d$ vs. 1/T was shown in Fig. 8. From the slope and intercept of the linear fitting, ΔH° and ΔS° were found to be –24.14 k J mol^{-1} and –77.55 J mol^{-1} K^{-1}, respectively. The Gibbs free energy (ΔGθ) was calculated from Eq. (7), its value was –1.38 kJ mol^{-1} when the adsorption temperature was 293.15 K. It indicated that BPA adsorption onto TiO_2-Mip-Ms was thermodynamically feasible and spontaneous.

3.6. The effect of coexisting pollutants on the recognition ability for BPA

In order to assess the effect of introduced phenyl group on the adsorption of BPA in complex matrix and the effect of BPA during preparation, adsorption experiment was carried out in binary solution systems containing 10 mg L^{-1} BPA and PP, or 10 mg L^{-1} BPA and 10 mg L^{-1} 2-NP, respectively. Fig. 9 depicts the equilibrium adsorption amounts of binary component of BPA and PP on TiO_2-Mip-Ms, TiO_2-Nip-Ms and TiO_2-Ms. The result indicated that the adsorption capacities for BPA onto TiO_2-Mip-Ms (8.65 mg g^{-1}) and TiO_2-Nip-Ms (8.98 mg g^{-1}) were higher than that of TiO_2-Ms (0.35 mg g^{-1}), and the adsorption capacities for PP onto TiO_2-Mip-Ms (0.68 mg g^{-1}) and TiO_2-Nip-Ms (0.69 mg g^{-1}) were relatively low. This result can be explained that the introduced phenyl group possessed hydrophobic property and had strong interaction with hydrophobic BPA through π-ϖ bond. The adsorption capacities for BPA and PP onto TiO_2-Ms were very low, because TiO_2-Ms possessed hydrophilic nature and hydrogen-bonding is very weak between hydroxyl

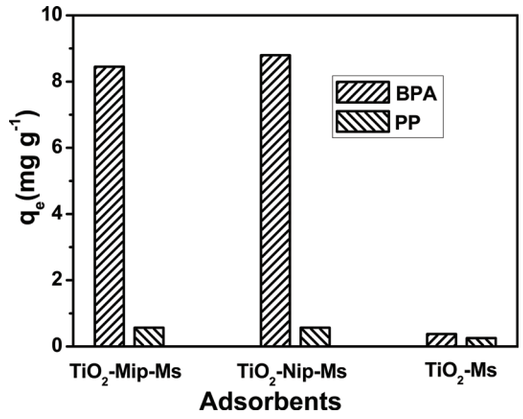

Fig. 9. Equilibrium adsorption capacities in binary component solution containing 10 mg L^{-1} BPA and 10 mg L^{-1} PP on three adsorbents.

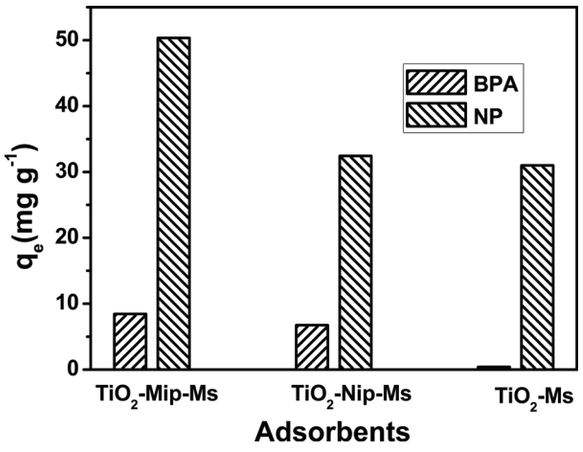

Fig. 10. Equilibrium adsorption capacities in binary component solution containing 10 mg L^{-1} BPA and 10 mg L^{-1} 2-Nitrophenol on three adsorbents.

groups at the surface of Ms and hydroxyl groups of BPA and PP in aqueous solution. We also selected the 2-NP as another co-pollutant because of its similar structure with BPA. The adsorption capacities of the binary component of BPA and 2-NP on the three adsorbents were shown in Fig. 10. We can see that TiO_2-Ms has higher adsorption capacities for 2-NP (30.5 mg g^{-1}) because the nitro-group of 2-NP has a stronger hydrogen-binding with TiO_2-Ms. It is interesting to find that 2-NP adsorption capacities onto TiO_2-Mip-Ms (50.0 mg g^{-1}) is nearly two times higher than that on TiO_2-Nip-Ms (32.2 mg g^{-1}), and the adsorption capacity for BPA remained unchanged (8.66 mg g^{-1}), which can be explained that 2-NP is somewhat similar to BPA in chemical structure, and it can diffuse easily into large cavities resulting from the BPA pore expanding agent. However, the adsorption capacity of BPA on TiO_2-Nip-Ms decreased correspondingly when 2-NP existed, because 2-NP can occupy the surface sites of TiO_2-Nip-Ms competitively with BPA.

4. Conclusions

A new type of phenyl-functionalized Ms based on TiO_2 supporter was successfully prepared via surface molecular imprinting technology combined with sol-gel method. The introduction of phenyl group and the existence of much more adsorption sites in Ms layer of TiO_2-Mip-Ms resulted in faster adsorption rate, higher adsorption capacities for BPA than TiO_2-Nip-Ms and TiO_2-Ms. The adsorption behaviors of the adsorbent for BPA belonged to the pseudo-second-order kinetic model and obeyed the Langmuir model. Adsorption process was endothermic and spontaneous.

Acknowledgment

This work was financially supported by the National Natural Science Foundation of China (No. 21463028) and Natural Science Foundation of Yunnan Province (2016FB014). The Basic Research Foundation of Yunnan Tobacco Industry Co. Ltd (2015FL05).

References

[1] I.R. Falconer, H.F. Chapman, M.R. Moore, G. Ranmuthugala, Endocrine-disrupting compounds: A review of their challenge to sustainable and safe water supply and water reuse, Environ. Toxicol., 21 (2006) 181–191.
[2] X. Peng, Y. Yu, C. Tang, J. Tan, Q. Huang, Z. Wang, Occurrence of steroid estrogens, endocrine-disrupting phenols, and acid pharmaceutical residues in urban riverine water of the Pearl River Delta, South China, Sci. Total Environ., 397 (2008) 158–166.
[3] H. Zhou, X.J. Zhang, Z.S. Wang, Research development of endocrine disrupting chemicals (EDCs) in water in China, Biomed. Environ. Sci., 16 (2003) 62–67.
[4] J.A. Rogers, L. Metz, V.W. Yong, Review: Endocrine disrupting chemicals and immune responses: A focus on bisphenol-A and its potential mechanisms, Mol Immunol., 53 (2013) 421–430.
[5] Z.H. Liu, Y. Kanjo, S. Mizutani, Removal mechanisms for endocrine disrupting compounds (EDCs) in wastewater treatment - physical means, biodegradation, and chemical advanced oxidation: A review, Sci. Total Environ., 407 (2009) 731–748.
[6] L.N. Vandenberg, R. Hauser, M. Marcus, N. Olea, W.V. Welshons, Human exposure to bisphenol A (BPA), Reprod. Toxicol., 24 (2007) 139–177.
[7] R.L. Gomes, M.D. Scrimshaw, J.N. Lester, Determination of endocrine disrupters in sewage treatment and receiving waters, TrAC-Trends in Analytical Chemistry, 22 (2003) 697–707.
[8] M. Petrovic, M. Sole, M.J.L. de Alda, D. Barcelo, Endocrine disruptors in sewage treatment plants, receiving river waters, and sediments: Integration of chemical analysis and biological effects on feral carp, Environ. Toxicol. Chem., 21 (2002) 2146–2156.
[9] I. Bautista-Toledo, M.A. Ferro-Garcia, J. Rivera-Utrilla, C. Moreno-Castilla, F.J. Vegas Fernandez, Bisphenol A removal from water by activated carbon. Effects of carbon characteristics and solution chemistry, Environ. Sci. Technol., 39 (2005) 6246–6250.
[10] Y.H. Kim, B. Lee, K.H. Choo, S.J. Choi, Selective adsorption of bisphenol A by organic–inorganic hybrid mesoporous silicas, Micropor. Mesopor. Mater., 138 (2011) 184–190.
[11] Y.L. Mao, H.Y. Kang, Y.F. Guo, S.T. Chen, Z.X. Wang, Synthesis of surface imprinted polymer upon modified kaolinite and study on the selective adsorption of BPA, Desal. Wat Treat., 57(9) (2016) 3947–3956.
[12] B.J. Lu, M.C. Liu, H.J. Shi, X.F. Huang, G.H. Zhao, A novel photoelectrochemical sensor for bisphenol A with high sensitivity and selectivity based on surface molecularly imprinted polypyrrole modified TiO_2 nanotubes, Electroanalysis, 25 (2013) 771–775.
[13] X. Hu, X.Wu, F.Yang, Q.Wang, C. He, S. Liu, Novel surface dummy molecularly imprinted silica as sorbent for solid-phase extraction of bisphenol A from water samples, Talanta, 148 (2016) 29–36.
[14] F. Hoffmann, M. Cornelius, J. Morell, M. Froeba, Silica-based mesoporous organic-inorganic hybrid materials, Angew. Chem. Int. Ed., 45 (2006) 3216–3251.
[15] X. Jiang, W. Tian, C. Zhao, H. Zhang, M. Liu, A novel sol–gel-material prepared by a surface imprinting technique for the selective solid-phase extraction of bisphenol A, Talanta, 72 (2007) 119–125.
[16] Y. Wang, Y. Yang, L. Xu, J. Zhang, Bisphenol A sensing based on surface molecularly imprinted, ordered mesoporous silica, Electrochim. Acta, 56 (2011) 2105–2109.
[17] W.Z. Xu, W. Zhou, P.P. Xu, J.M. Pan, X.Y. Wu, Y.S. Yan, A molecularly imprinted polymer based on TiO_2 as a sacrificial support for selective recognition of dibenzothiophene, Chem. Eng. J., 172 (2011) 191–198.
[18] T. Kimura, M. Suzuki, M. Maeda, S. Tomura, Water adsorption behavior of ordered mesoporous silicas modified with an organosilane composed of hydrophobic alkyl chain and hydrophilic polyethylene oxide groups, Micropor. Mesopor. Mater., 95 (2006) 213–219.
[19] S.R. Carter, S. Rimmer, Surface molecularly imprinted polymer core-shell particles, Adv. Funct. Mater, 14 (2004) 553–561.
[20] S. Lagergren, About the theory of so-called adsorption of soluble substances, Kungliga Svenska Vetenskapsakademiens Handlingar, 24 (1898) 1–39.
[21] Y.S. Ho, Thesis, The University of Birmingham, UK (1995).
[22] Y.S. Ho, G. McKay, A comparison of chemisorption kinetic models applied to pollutant removal on various sorbents, Process Saf. Environ. Prot., 76 (1998) 332–340.
[23] G. McKay, Use of Adsorbents for the Removal of Pollutants from Wastewaters, in: G. McKay (Ed.), ch. 7 – CRC Press, Boca Raton, FL, 1996.
[24] E. Alver, A.Ü. Metin, Anionic dye removal from aqueous solutions using modified zeolite: Adsorption kinetics and isotherm studies, Chem. Eng. J., 200–202 (2012) 59–67.
[25] F. An, B. Gao, X. Feng, Adsorption and recognizing ability of molecular imprinted polymer MIP-PEI/SiO_2 towards phenol, J. Hazard. Mater., 157 (2008) 286–292.